www.arpnjournals.com

REGIONAL ATROPHY ANALYSIS OF ALZHEIMER BRAIN MAGNETIC RESONANCE IMAGES USING LOCAL TEXTURE PATTERNS

A. Sakthi Bharathi[1] and D. Manimegalai[2]
[1]Department of Computer Science Engineering, University VOC College of Engineering, Tuticorin, India
[2]Department of Computer Science Engineering, National Engineering College, Kovilpatti, India
E-Mail: v_sakthibharathi@yahoo.co.in

ABSTRACT

Alzheimer Disease (AD) is the most common type of dementia among elderly people. It is a severe neurodegenerative disorder which is highly characterized by progressive loss of brain tissues. It interferes with normal activity of daily living due to loss of cognitive ability. Magnetic Resonance Imaging (MRI) has been proven to be very useful in early diagnosis and progression analysis of AD. This paper investigates the regional atrophy due to Alzheimer disease progression in four common brain tissues such as Cerebro Spinal fluid (CSF), Ventricle Segment (VS), White Matter (WM) and Gray Matter (GM) using their corresponding local texture patterns. The extracted information is used to classify Normal, Mild Cognitive Impaired (MCI) and AD subjects. An attempt is made to automatically segment the common brain tissues like WM, GM, CSF and VS. Features are extracted from their local texture patterns. Classification of Normal, MCI and AD is performed in order to investigate the efficiency of these extracted features as biomarkers in automated analysis of Alzheimer diagnosis. Anisotropic Diffusion filter based Level Set Method (ADLSM) is adapted to segment GM, WM, CSF and VS regions of brain. Fuzzy C means Clustering (FCM) technique is used to draw the initial contour which is later evolved using level set contour towards the desired boundaries. Local texture patterns such as Local Binary Patterns (LBP), Local Tetra Patterns (LTrP), Local Ternary Patterns (LTP) and Local Maximum Edge Binary Patterns (LMEBP) of segmented images are calculated. Histogram based features are extracted from these local patterns in order to classify NC, MCI and AD. It shows that the proposed FCM based ADLSM could able to segment the various brain tissues accurately. All local patterns are able to bring out the structural variations in terms of edge details. A maximum accuracy of 100 % is observed using LTP features and SVM classifier in differentiating AD and normal in GM, WM and whole brain regions. LMEBP features show an average performance measure of greater than 75% accuracy in differentiating MCI and normal subjects using SVM classifier. Similarly, LTP features show a good performance measure of 100% classification accuracy in differentiating AD and MCI in whole brain region. In conclusion, histogram features derived from local ternary patterns could be an efficient biomarker for classification of AD, MCI and normal subjects. Textural variations in gray matter and whole brain regions contribute more in differentiating the disease progression using local patterns. Hence, the proposed flow of segmentation algorithm, LTP feature extraction of various brain tissues along with SVM classifier may help to improve the automated diagnosis of Alzheimer disease progression.

Keywords: alzheimer, magnetic resonance imaging, local binary, ternary and tetra patterns, local maximum edge based binary patterns, anisotropic diffusion filter, level set method.

1. INTRODUCTION

Dementia is a chronic and progressive syndrome which deteriorates the cognitive function especially in aged people, worldwide. It affects memory, thinking, behaviour and the ability to perform everyday activities. It is estimated that 47.5 million people worldwide are affected with dementia, reporting 7.7 million new cases every year. It is also predicted that 75.6 million people will be affected by 2030 and almost triple by 2050. One of the most common forms of dementia is Alzheimer Disease (AD) which is a neuro-degenerative disorder and it accounts for 60 % - 70 % of dementia cases [1].

Currently, there are no treatments available to cure AD or alter its progressive nature. But, it is reported that the early diagnosis of AD can help to provide more information for treatment planning and long - term support for dementia care [1, 2]. The standard procedure of diagnosing AD requires brain tissue samples, which may be obtained either by autopsy or brain biopsy. Mini mental score examination and clinical dementia ratio are the two common clinical tests that are used currently for diagnosis of AD [3]. Mild cognitive Impairment (MCI) is a new transitional stage from normal to AD. It is defined as a stage when a patient has some mild memory loss problem but still can do their day to day activities. It is reported that there is a high risk of converting MCI to AD cases and 50% of MCI patients convert to AD in a period of three years [4].

The brain tissues of AD patients are characterized by amyloid plaques and neurofibrillary changes, hippocampal atrophy, gray and white matter atrophy due to neuronal losses and enlargement of ventricle and sulci [5-9]. Normal brain parts are categorized mainly as cerebrospinal fluid (CSF), white matter (WM) and gray matter (GM). CSF is located between the brain and skull and it is liquid part of the brain. It is reported that enlarged CSF area can be potential indicator of AD patients [10]. Ventricle Segment (VS) is defined as an empty space within cerebral hemisphere and brain stem and is filled with CSF liquid. In AD patients, ventricle is identified as

www.arpnjournals.com

an enlarged region with increased volume. It can also be a bio-marker in AD analysis [11, 12]. Gray matter is one of two major tissues in the brain. It consists of cell bodies of neural system. The degeneration of this structure in various parts is highly related to AD progression. Various studies have been reported about white matter abnormalities related to AD diagnosis. Temporal lobe WM atrophy is treated as one of important bio-marker in evaluating AD prognosis [9, 13].

The neuro imaging modalities such as Computed Tomography (CT), Single-Photon Emission Computed Tomography (SPECT) and Positron Emission Tomography (PET) have confirmed the GM tissue losses, abnormalities in WM and increase CSF [9]. Either GM or WM loss or even the combination of both may lead to brain atrophy. As dementia is primarily attributed due to neuronal loss, greater extent of brain tissue loss is expected to happen in GM than WM. Several investigations have reported that WM is secondarily affected brain tissue region in AD patients. Two ways of brain tissue analysis have been reported in the literature. First, volume analyses in which whole or specific regions of the brain are quantified with manual tracing. Second, the amount of various brain tissue types namely GM, WM, VS and CSF are quantified based on segmentation and pixel intensity based features [9, 10].

Clinically, Magnetic Resonance Imaging (MRI) of brain is reported as an efficient non-invasive diagnosis of neuro degenerative disorders [14]. It is an imaging technique that has high spatial resolution. Structural changes in the brain that are associated with AD can be non-invasively assessed using MRI. The brain tissue reduction in AD is primarily captured on MR brain images due to signal loss in the cortex, medical temporal lobe and enlarged cerebrospinal fluid and ventricles. This help to visualize atrophy in different views [15]. Hence, MR imaging is widely used for AD diagnosis when compared to other modalities such as CT, SPECT and PET. Most of recent research aims to compare biological, neuro imaging and clinical assessment of behavioural and cognitive changes induced due to normal ageing, MCI and AD [16].

The simplest approach to identify regional changes in brain is visual voting and it helps to compare the atrophy level in MR images. It is reported that the accuracy of this method is around 89% in classifying AD and normal subjects [17]. High degree of atrophy is reported in sub-regions of medical temporal lobe during mild stages of AD and neocortical and cortical regions in the advanced AD stages [18]. On set of dementia happens several years before and hence, these atrophy patterns can be detected at early stages of AD and MCI using MRI scans. It is also reported that the manual measurement of hippocampus and entorhinal cortex volumes has given an accuracies around 80% to 85% in predicting the disease progression from MCI to AD [19]. The manual segmentation of region of interest is time consuming, highly variable from person to person and prone to errors.

Identification of potential biomarkers for early diagnosis of AD is important in order to enhance the diagnosis, monitoring and drug delivery. Therefore, there is a need for automated image based classification of individual patients to support the clinicians. This limits the manual segmentation of atrophy analysis in general neuro degenerative disorders [20]. Hypotheis driven automated approaches to segment hipoocampus volume reached accuracies around 70% to 80% in differentiating MCI and AD subjects from normal subjects [21]. The diagnostic accuracy of classifying AD, MCI from normal subjects have increased to 90% when combination of several neuro anatominal ROI regions is considered [22]. Data driven approaches are introduced where the local differences in the brain tissues are used [23].

The studies based on ventricle enlargement are reported for neurodegenerative disorders. It is reported as a significant biomarker for identification of AD, MCI and normal subjects [11]. The ventricle shape has been used to differentiate AD and normal subjects and an accuracy of 84% has been reported [12]. As the volume analysis is time consuming procedure, in 1998, Peter A. Freeborough et al. [24] used texture analysis to diagnose AD and reported with a classification rate of 91%. There are studies that emphasise the importance of texture analysis using gray level dependence, gray level non uniformity and run length non uniformity for classification among AD, MCI and Normal subjects [25]. It is reported that texture analysis showed a significant variation and hence, aided for early detection of brain related disorders.

Local Binary Patterns (LBP), a texture descriptor is introduced as a powerful feature in classifying dementia using MR brain images [26]. Later in 2012, it has been reported that LBP, contrast features and white matter volume as an efficient biomarker in classifying dementia using WM of brain MR images [27]. It is also reported that LBP and its contrast measure as a potential feature to classify the whole brain MR images into three classes of dementia [28].

First step towards automated analysis of Alzheimer disease using MR images is to extract the brain tissue region. The segmentation of brain MRI remains to be a challenging in neuro imaging studies [29]. Several segmentation algorithms have been reported which includes thresholding, atlas guided approaches, clustering, markov random fields models and deformable models. Gradient vector flow snakes and level set methods are two deformable modeling techniques that have been reported and used to segment brain tissues from MR images [30]. The drawbacks of deformable models are energy optimization problem and different results being generated with different initial contours for the same image. Therefore, edge based level set method are proposed in which the initial level set contour is evolved using edge maps. These edge maps are derived as the inverse gradient of the Gaussian smoothed images. Due to thick and spurious edges, the level set contour tends to settle in false edge boundaries which is so critical in case of medical

imaging. To address this issue, Suganthi *et al.* introduced anisotropic diffusion filter based level set method to segment breast thermal images [31]. By using non linear filter, the edge details are preserved and resulted with thin and clear edge boundaries. The initial contours are derived manually. ADLSM is also reported for extraction of VS and atrophy analysis of corpus callosum regions in AD brain MR images. It is reported that ventricle extraction and its morphology changes are potential biomarkers for AD diagnosis [32, 33]. Fuzzy C Means (FCM) clustering technique has been reported for automated segmentation and volume analysis of WM, GM and CSF regions of brain MR images [34]. Integration of FCM and conventional LSM is widely used and reported to extract brain tissue regions, skin lesions and blood vessels in angiograms [35, 36].

In this study, the potential of local texture patterns of regional brain tissues as features and as Alzheimer biomarkers are studied using MR images. In the following, the major anatomical parts of brain tissues like gray matter (GM), white matter (WM), Cerebrospinal fluid (CSF) and Ventricle Segment (VS) are evaluated in terms of their discriminative power in classifying the subjects into different pairs of populations (AD vs MCI, MCI vs Normal, AD vs Normal and AD vs MCI vs Normal). The analysis on whole brain (WB) is also carried out. The various regions of the brain tissues are segmented using FCM and anisotropic diffusion filter based level set. The local patterns namely local binary patterns (LBP), local ternary patterns (LTP), local tetra patterns (LTrP) and local maximum edge binary patterns (LMEBP) of each segmented brain regions are obtained. From each pattern, histogram based features like mean, variance, skewness, kurtosis, energy, entropy and few shape based features are extracted. These feature vectors are used to classify the subjects into AD, MCI and normal using four different classifiers like naive bayes, support vector machine, adaboost and random forest. The obtained results and the corresponding discussions are presented in this paper.

2. METHODOLOGY

2.1 Image database

The proposed segmentation and feature extraction methods are experimented on brain MR images that are obtained from online databases Open Access Series of Imaging Studies (OASIS) [37]. They are T1 - weighted images of resolution 1.0 x 1.0 x 1.25 mm^3. MR brain images of 90 subjects are considered in this work. Based on Clinical Dementia Rating (CDR) values the images are grouped such as 30 subjects in Normal (CDR = 0), 30 subjects in Mild cognitive impaired (CDR = 0.5) and 30 subjects in Alzheimer disease condition (CDR >=1). These subjects are all right-handed and aged on an average of 78±6.91 (AD), 76.21±7.18 (MCI) and 69.07±13.87 (Normal). This set of data include both men and women subjects of AD, MCI and NC as 20F/10M, 39F/31M and 97F/38M respectively. These images are gain-field corrected and atlas registered and hence it is ensured that the voxels in different images refer to same anatomical positions of the brain.

2.2 Anisotropic diffusion filter based level set method

The variational level set method without reinitialization [38] proposed by Li *et al.* which is an active contour method uses a Gaussian filtered image as an edge map for the initial contour to evolve towards the boundary. As it is a linear diffusion and homogenous filter, it blurs and thickens the edges and hence, the level set contours may evolve towards the false boundaries. In this work, a non-linear isotropic diffusion filter based level set method without reinitialization is used to segment the Gray Matter (GM), White Matter (WM), Cerebro Spinal Fluid (CSF) and Ventricle Segment (VS) of the brain [31, 32]. The initialization of zeroth level set is automated using Fuzzy C means Clustering algorithm.

The general form of curve evolution equation of level set function is given by the gradient flow equation as [38].

$$\frac{\partial \varphi}{\partial t} = \mu[\Delta\varphi - div(\nabla\varphi/|\nabla\varphi|)] + \lambda\,\delta(\varphi)div(g\,\nabla\varphi/|\nabla\varphi|) + \nu g\,\delta(\varphi) \tag{1}$$

where μ, λ are constants, φ indicates the initial contour and g represents the edge map function of the image and helps the initial contour to evolve to desired boundary. If I represents the original raw brain MR image, I_t represents the non linear isotropic diffusion filtered image and the edge map g is defined as [31].

$$g = \frac{1}{1+|\nabla I_t|^2} \tag{2}$$

To segment the various brain tissues such as GM. WM, and CSF, the respective initial contours are given automatically using Fuzzy C means Clustering algorithm. It is an unsupervised technique in which the image is

represented in various feature spaces, and the related data points in this feature space is grouped into clusters. This is achieved by minimizing a cost function which is directly related to the distance between the pixels and cluster centres in the feature domain. The cost function that is minimized iteratively is given as [39].

$$J = \sum_{i=1}^{N}\sum_{j=1}^{c} u_{ij}{}^{m}\left\|x_j - v_i\right\|^2 \tag{3}$$

where m is a constant that controls the fuzzy nature of the partition, $\|.\|$ represents the norm function, u_{ij} represents the membership function of pixel x_j in the ith cluster and is defined as:

$$u_{ij} = \frac{1}{\sum_{k=1}^{C}\left(\frac{\|x_j - v_i\|}{\|x_j - v_k\|}\right)^{2/(m-1)}} \quad (4)$$

and v_i is the ith cluster center defined as

$$v_i = \frac{\sum_{j=1}^{N} u_{ij}{}^m x_j}{\sum_{j=1}^{N} u_{ij}{}^m} \quad (5)$$

There is a probability that in an image, the neighbouring pixels posses similar feature values and belong to same cluster as they are highly correlated Exploiting this spatial correlation of pixels, the spatial function is defined as

$$h_{ij} = \sum_{k \in NB(x_j)} u_{ik}, \quad (6)$$

where $NB(x_j)$ is a square window centered on pixel x_j in the spatial domain. This function for a cluster results as a large value if the majority of its neighbourhood pixel belongs to same clusters. The membership function is then given as

$$u_{ij}' = \frac{u_{ij}{}^p h_{ij}{}^q}{\sum_{k=1}^{C} u_{kj}{}^p h_{kj}{}^q} \quad (7)$$

Where p and q are constants used to control the relative importance of both functions. It is performed as a two pass process at each iteration. Standard membership function is used to calculate during first pass. Spatial function is computed in the second pass by mapping the membership information to spatial domain pixels. Thus new membership function is computed and iteration proceeds till the maximum difference between two clusters at two successing iterations is less than a threshold. After the convergence, defuzzification is performed by assigning each pixel to a specific cluster for which the membership is maximal.

2.3 Feature extraction

Histogram based local texture features, global features such as non-zero pixel area, entropy and shape based features are calculated from these segmented images and their performance as an efficient biomarker in differentiating normal, MCI and AD is analyzed.

2.3.1 Local Binary Pattern (LBP)

Local Binary Patterns was first proposed by Ojala et al. [40] for texture classification. Later, LBP was attracted by many research areas due to its performance in terms of speed. Other areas in which LBP was used and reported are face recognition, object tracking, content based image retrieval, biomedical and finger print recognition [41]. The local binary pattern is a texture

feature that is computed given a centre pixel g_c governed by the following equation.

$$LBP_N = \sum_{n=1}^{N} 2^{(n-1)} \times f_1(g_n, g_c) \,|_{N=8} \quad (8)$$

$$f_1(g_n, g_c) = \begin{cases} 1, & \text{if } g_n - g_c \geq 0 \\ 0, & \text{otherwise} \end{cases} \quad (9)$$

where N is the number of neighborhood pixels of radius 1 (chosen for this study) and g_n is the gray value of the neighbor pixel.

2.3.2 Local Ternary Pattern (LTP)

The local ternary pattern is a texture feature that returns two sets of binary values computed as follows [42].

$$LTP1_P = \sum_{n=1}^{N} 2^{(n-1)} \times f_2(g_n, g_c, t) \quad (10)$$
$$f_2(g_n, g_c, t) = \begin{cases} 1, & \text{if } g_n \geq g_c + t \\ 0, & \text{otherwise} \end{cases}$$

$$LTP2_P = \sum_{n=1}^{N} 2^{(n-1)} \times f_3(g_n, g_c, t)$$
$$\qquad (11)$$
$$f_3(g_n, g_c, t) = \begin{cases} -1, & \text{if } g_n \leq g_c - t \\ 0, & \text{otherwise} \end{cases}$$

where, t is the threshold that helps in eliminating the effect of noises present in the images.

2.3.3 Local Tetra Pattern (LTrP)

LTrP is extended version of LBP and derived from the concepts of LBP and LTP. It defines the local pattern according to the direction of centre pixel [43].

The first order derivative along $0°$ and $90°$ is represented as

$$I_{0°}^{1}(g_c) = I(g_h) - I(g_c) \quad (12)$$

$$I_{90°}^{1}(g_c) = I(g_v) - I(g_c) \quad (13)$$

Where g_h represents the horizontal neighboring pixel to the center pixel g_c and g_v represents vertical neighboring pixel, $I_{\theta°}^{1}$ represents the first order derivative of the image along $\theta°$. The direction of the center pixel is defined as:

$$I_{Dir}^{1}(g_c) = \begin{cases} 1, & I_{0°}^{1}(g_c) \geq 0 \text{ and } I_{90°}^{1}(g_c) \geq 0 \\ 2, & I_{0°}^{1}(g_c) < 0 \text{ and } I_{90°}^{1}(g_c) \geq 0 \\ 3, & I_{0°}^{1}(g_c) < 0 \text{ and } I_{90°}^{1}(g_c) < 0 \\ 4, & I_{0°}^{1}(g_c) \geq 0 \text{ and } I_{90°}^{1}(g_c) < 0 \end{cases} \quad (14)$$

The second order LTrP is defined as follows,

$$LTrP^2(g_c) = \{f_4(I_{Dir}^{1}(g_c), I_{Dir}^{1}(g_1)), f_4(I_{Dir}^{1}(g_c), I_{Dir}^{1}(g_2)), \dots f_4(I_{Dir}^{1}(g_c), I_{Dir}^{1}(g_N))\}|_{N=8}$$
$$(15)$$

$$f_4(I_{Dir}^1(g_c), I_{Dir}^1(g_n)) = \begin{cases} 0, & I_{Dir}^1(g_c) = I_{Dir}^1(g_n)) \\ I_{Dir}^1(g_n), & \text{otherwise} \end{cases} \qquad (16)$$

Let's assume that for a particular $g_c = 1$, the $LTrP^2$ can be refined into corresponding binary patterns as follows:

$$LTrP^2|_{\emptyset=2,3,4} = \sum_{n=1}^{N} 2^{(n-1)} \times f_5(LTrP^2(g_c), \emptyset) \qquad (17)$$

$$f_5(LTrP^2(g_c), \emptyset) = \begin{cases} 1, \text{if } LTrP^2(g_c) = \emptyset \\ 0, \text{othewise} \end{cases} \qquad (18)$$

The tetra pattern includes a magnitude pattern extracted as given below

$$M_{I^1(g_n)} = \sqrt{I_{0°}^1(g_n)^2 + I_{90°}^1(g_n)^2} \qquad (19)$$

The magnitude pattern is given by,

$$MP = \sum_{n=1}^{N} 2^{(n-1)} \times f_1(M_{I^1(g_n)}, M_{I^1(g_c)}) |_{N=8} \qquad (20)$$

2.3.4 Local Maximum Edge Binary Patterns (LMEBP)

Local Maximum Edge Binary Patterns (LMEBP) was proposed for image retrieval and object tracking applications [41]. It is reported that LMEBP captures more edge information when compared to LBP. LMEBP of an image is calculated as the magnitude of the local difference between the centre pixel and its eight neighbours. The obtained local differences are arranged in descending order representing first maximum edge to eighth maximum edge. Each edge is assigned as either '1' or '0' based on the local difference. A binary value of '1' is assigned when the value is greater than or equal to zero, '0' otherwise. Finally, first maximum edge to eight maximum edge is coded based on nine binary values. The algorithm is implemented using the following equations:

$$I'(g_i) = I(g_i) - I(g_c), i = 1,2,..., 8 \qquad (21)$$

$$I_i = \arg(\max(|I'(g_1)|, |I'(g_2)|, ... |I'(g_8)|)) \qquad (22)$$
where max(x) returns the maximum value of x.

A binary value is assigned based on the edge value. If the edge is positive, '1' is assigned and '0' otherwise. Therefore,

$$I_{new}(g_c) = f(I'(g_{i1})) \qquad (23)$$

f (x) = 1, x >= 0,
0, else
LMEBP is defined as

$$LMEBP(I(g_c)) = \{I_{new}(g_1), I_{new}(g_2), ..., I_{new}(g_8)\}. \qquad (24)$$
whose values range from 0 to 511.

2.4 Classification

Histogram features such as mean, variance, skewness; kurtosis, energy and entropy are calculated from each segmented brain tissues and obtained binary patterns. Feature vector is formed using the histogram features of the corresponding brain tissue and its local patterns. In case of LBP, the feature vector size is 12. LTP results in two binary images and hence, the feature vector size is 18 (2 * 6 + 6). Similarly, LTrP results in 4 binary images and the feature vector size is 30 (4 * 6 + 6). Finally, LMEBP results in 8 binary patterns and hence, the size of feature vector is 54 (8 * 6 + 6). As ventricle is characterized by increased shape during AD progression, additionally, shape based features are extracted. Therefore, for ventricle analysis, the feature vector includes the corresponding defined histogram features set and shape based features (x + 7, x belongs to feature set based on LBP/LTP/LTrP/LMEBP). The additional shape based features include area, perimeter, 5 shape factors. The five shape factors are derived from the basic geometric descriptors like area, perimeter and axis length. It is defined as [44].

$$Shape\ factor\ 1 = \frac{1}{compactness} \qquad (25)$$

$$Shape\ factor\ 2 = \frac{Major\ axis\ length}{Area} \qquad (26)$$

$$Shape\ factor\ 3 = \frac{Area}{Major\ axis\ length^3} \qquad (27)$$

$$Shape\ factor\ 4 = \frac{Area}{\left(\left(\frac{Major\ axis\ length}{2}\right)*\left(\frac{Major\ axis\ length}{2}\right)*pi\right)} \qquad (28)$$

$$Shape\ factor\ 5 = \frac{Area}{\left(\left(\frac{Major\ axis\ length}{2}\right)*\left(\frac{Minor\ axis\ length}{2}\right)*pi\right)} \qquad (29)$$

2.5 Performance evaluation

The significance of the extracted features are studied by differentiating the samples as AD, MCI and Normal using four different classifiers in order to

understand the effectiveness of these feature sets. The classifiers used are Naive Bayes, Support Vector Machine, AdaBoost and Random Forest. The proposed analysis is divided into four groups in which three are binary classification problems and one being a three class problem. In case of binary classification, we attempted to classify AD and MCI, MCI and Normal and finally, AD and Normal. In three class problem, we attempted to classify AD, MCI and Normal samples. The performance of the extracted features and classifier is analysed by calculating the evaluation metrics namely Accuracy, Specificity and Sensitivity. These metrics are derived based the confusion matrix.

This study is performed by extracting the features using LBP, LTP, LMEBP and LTrP patterns. Further, these features are extracted from whole brain regions and also from various brain regions such as White matter, Grey matter, cerebrospinal fluid and ventricle. The feature set from a particular region that resulted in maximum accuracy is reported, discussed and proposed for the analysis of Alzheimer Disease using MR brain images.

3. RESULTS AND DISCUSSIONS

The experimental performance of the proposed analysis of Alzheimer disease using MR brain images is discussed in this section. Skulled stripped whole brain tissue region and various regions like gray matter (GM), white matter (WM), cerebrospinal fluid (CSF), and Ventricle Segment (VS) are segmented using anisotropic diffusion filter based level set method and Fuzzy C means clustering algorithm. Histogram features from local patterns like local binary patterns (LBP), local ternary patterns (LTP), local maximum edge binary patterns (LMEBP) and local tetra patterns (LTrP) are extracted. The performance of these features in differentiating Alzheimer Disease (AD), Mild Cognitive Impairment (MCI) and Normal images are analysed using four different classifiers such as naive bayes (NB), support vector machine (SVM), Adaboost (AB) and Random forest (RF) methods. The obtained results at various stages are displayed and discussed in this section.
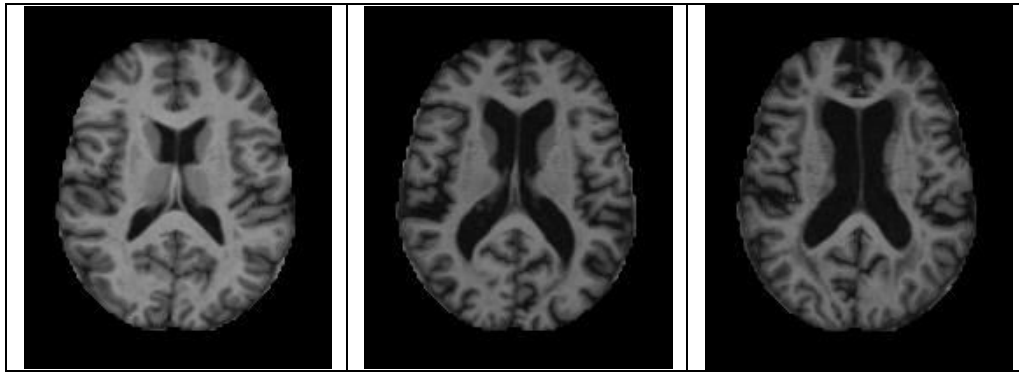
Figure-1 represents typical brain MR images of normal, MCI and AD subjects with and without skull region. Skull stripped brain images are obtained from the database and is used for whole brain region analysis. The difference in brain tissue losses in terms of structural and textural information can be easily visualized among normal, MCI and AD subjects. The VS region seems to be enlarged due to the disease progression.

| Normal | MCI | AD |
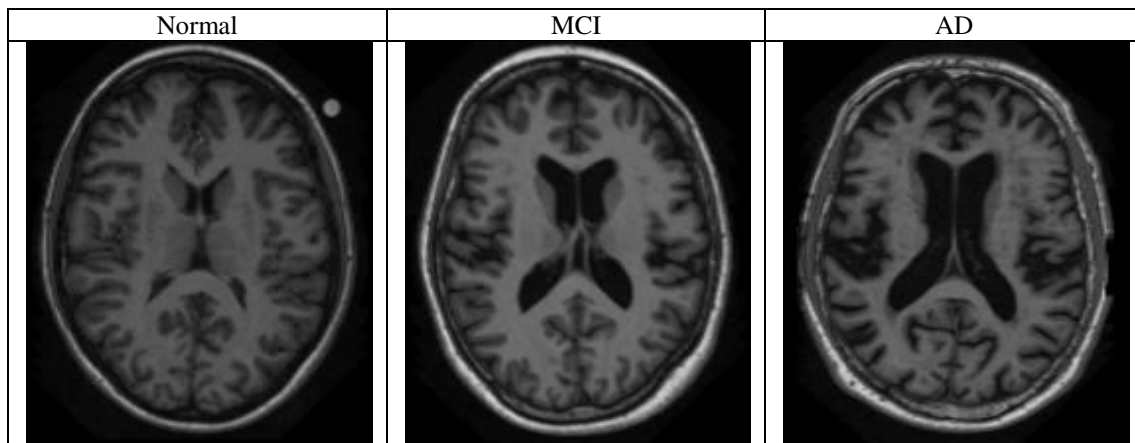
Figure-1. Typical brain MR images of normal, mild cognitive impairment and Alzheimer disease.

Figure-2 depicts the representative images of normal, AD and MCI subjects after skull stripping. It shows only the brain tissue regions. The intensity variations can be observed for CSF, GM and WM in an increasing order representing CSF as dark gray regions. The centre region is ventricle which is filled with CSF and carries very low intensity values. The texture difference between AD, MCI and normal images can be easily visualized from these images. The enlarged ventricle region indicates the progression of AD. The difference in the intensity variations is prominent in MCI and AD subjects compared to normal subjects. This may be due to brain tissue loss or shrinkage of brain regions resulted with increased CSF regions.

www.arpnjournals.com

Figure-2. Typical brain MR images of normal, mild cognitive impairment and
Alzheimer disease.

The skull stripped images are subjected to segmentation procedure using anisotropic diffusion filter based level set method. The level set method uses edge map of the brain tissues in order to evolve the initial contour. In conventional level set method, the edge map is obtained using Gaussian filtered image and is shown in Figure-3. Level set contour may get confused between the true and false boundaries due to presence of thick and spurious edges as shown in Figure-3(b). Therefore, the final segmented image may not the desired region of interest (ROI) and may lead to increased false positive results. This is addressed by replacing Gaussian filter as anisotropic diffusion filter which is a non linear filter. The filter performs non linear filtering operation and hence, the edge details are preserved. This can be clearly observed from Figure-3(c). The initial contour for the level set method to evolve is obtained as clusters using Fuzzy C means Method (FCM) to segment the brain regions as CSF, WM and GM.

(a)   (b)   (c)
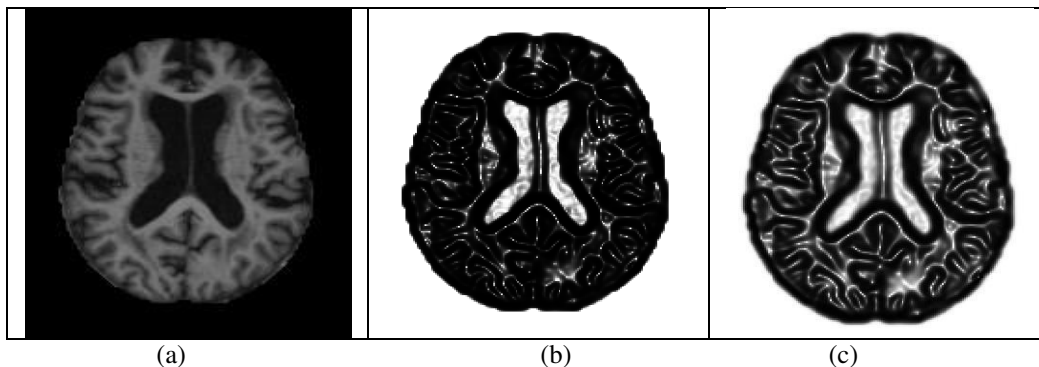
Figure-3. Typical edge maps of brain MR images (a) Original image (b) Gaussian filter
based edge map (c) Non linear isotropic filter based edge map.

Figure-4 represents the intermediate results obtained during the segmentation of various brain regions. It show the results of FCM clustering technique, initial contour, final contour, segmented mask and corresponding segmented images. The initial segmentation is performed using FCM technique. The obtained segmented clusters through FCM are used as initial contours for the level set to evolve towards desired boundary. It is seen that the initial contours gave a rough estimate of region boundaries. The exact boundary is achieved by evolving the initial contour based on the edge map over minimum iteration. The final evolved contour shows that the anisotropic diffusion level set method based segmentation algorithm could effectively segment the regions accurately. The segmented mask is generated as the result of segmentation and segmented image is obtained by multiplying the mask with raw image.

www.arpnjournals.com

Cluster	Initial Contour	Final Contour	Segmented Mask	Segmented Image
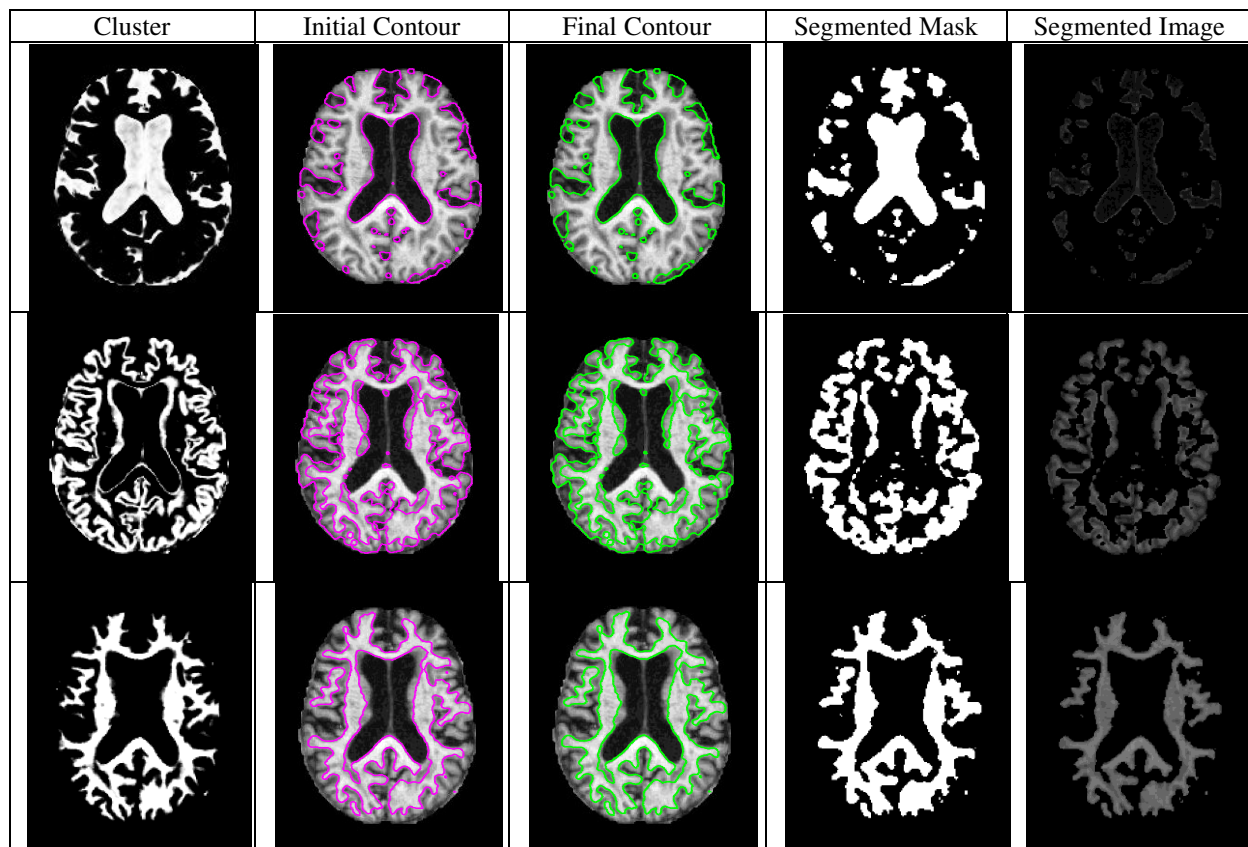
Figure-4. Typical segmentation results of various brain tissues using non linear isotropic diffusion filter based level set method. First Row: Cerebro Spinal Fluid, Second Row: Gray Matter, Third Row: White Matter.

The ventricle segmentation is performed using anisotropic diffusion filter based level set method. The initial contour, final contour, segmented mask and segmented images are shown in Figure-5. The initial contour is given manually inside the ventricle region and is evolved according to the edge map. The results obtained shows that the segmentation method is able to accurately segment the ventricle region.

Skull stripped Image	Initial Contour	Final Contour	Segmented Mask	Segmented Image
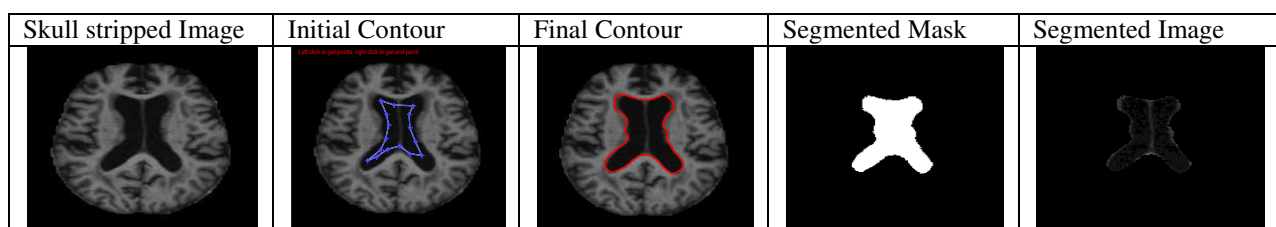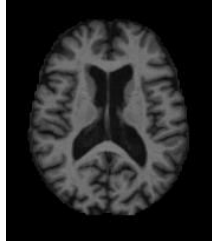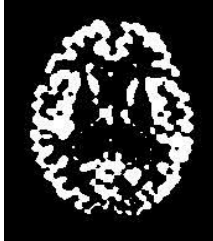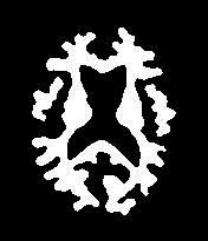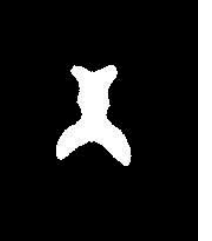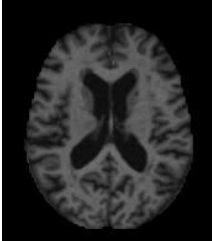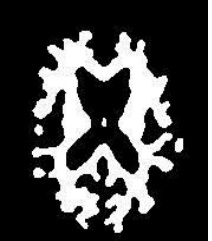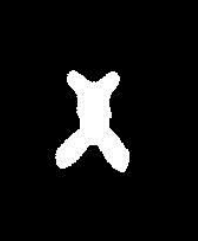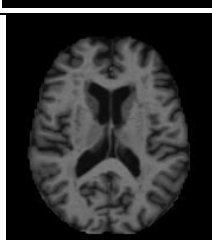
Figure-5. Typical segmentation results of Ventricle using non linear isotropic diffusion filter based level set method.

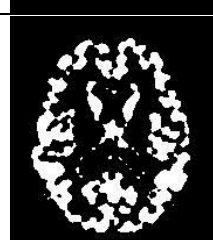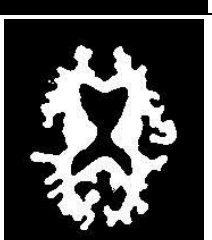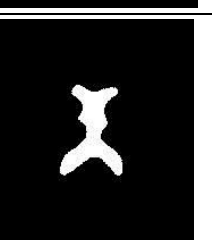Typical results of segmented GM, WM, CSF and Ventricle regions are shown for normal, AD and MCI images in Figure-6. It shows that the FCM based ADLSM is capable of segmenting the various brain regions irrespective of pathological conditions. LBP, LTP, LTrP and LMEBP images are derived from the segmented GM, WM, CSF and Ventricle regions. The same is also performed on whole brain regions. Histogram based features are calculated and feature vector is formed. Figure-7 shows the scatter plot of calculated area of segmented ventricle as feature. It shows that the ventricle area of AD subjects is greater than normal subjects and this feature can be an efficient biomarker for classifying AD and normal subjects. As MCI is a transition form from normal to AD, the ventricle areas are found to be scattered sharing both normal and AD subjects.

481

www.arpnjournals.com

Figure-6. Typical segmentation results of cerebro spinal fluid, gray matter and white matter of varied pathological conditions of brain tissues.

Figure-7 shows a scatter plot representation of area as a significant feature of the segmented ventricle across normal, MCI and AD subjects. A gradual increase in the ventricle area is observed as disease progresses. The ventricle area of the normal subject is significantly lower than AD subjects. In case of MCI, the area falls in between the normal and AD subjects. It shows significant overlap with both the normal and AD subjects. It can be seen that the disease progresses, the ventricle area enlarges. The same pattern is observed for other shape based features as well.
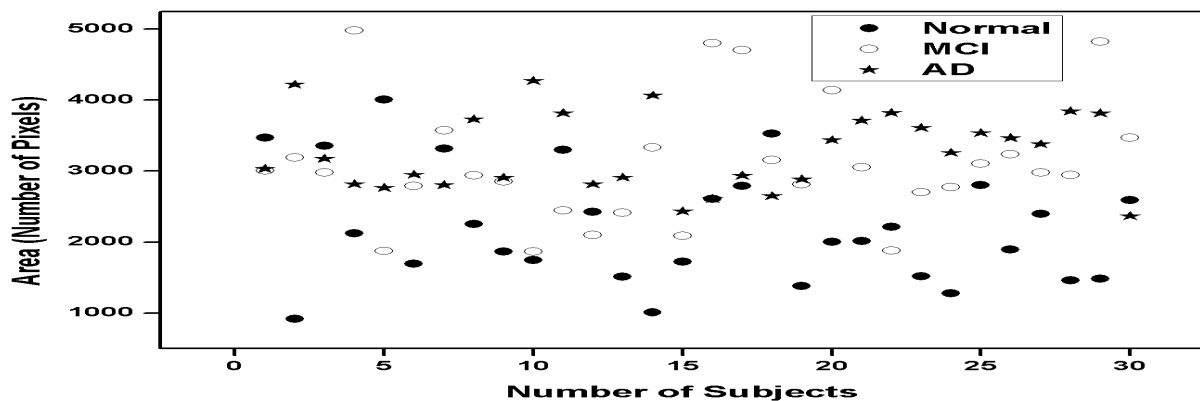
Figure-7. Scatter plot diagram of the feature area of segmented ventricle.

The extracted histogram features and shape based features are formed into the corresponding feature vectors and are used to classify the MR brain images into normal, AD and MCI. The performance of different classifiers for these extracted features is analyzed. The results using LTP feature vector show maximum performance of 100% for Gray matter and whole brain regions using NB classifier in differentiating AD and MCI subjects. The obtained values are shown in Table-1.

Table-1. Classification results using Naive Bayes and LTP features for differentiating AD and MCI.

|	CSF	GM	WM	VS	WB
Accuracy	**0.683**	**1**	**0.617**	**0.567**	**1**
Sensitivity	0.739	1	0.652	0.60	1
Specificity	0.649	1	0.595	0.55	1

As the whole brain and gray matter regions have more texture when compared to other regions, they showed the maximum accuracy in classifying AD and MCI. Ventricle regions show comparatively less accuracy which may be due to the homogenous area and negligible texture information is present. The classification accuracy of different local patterns using different classifiers for all brain regions is shown in Figure-8.
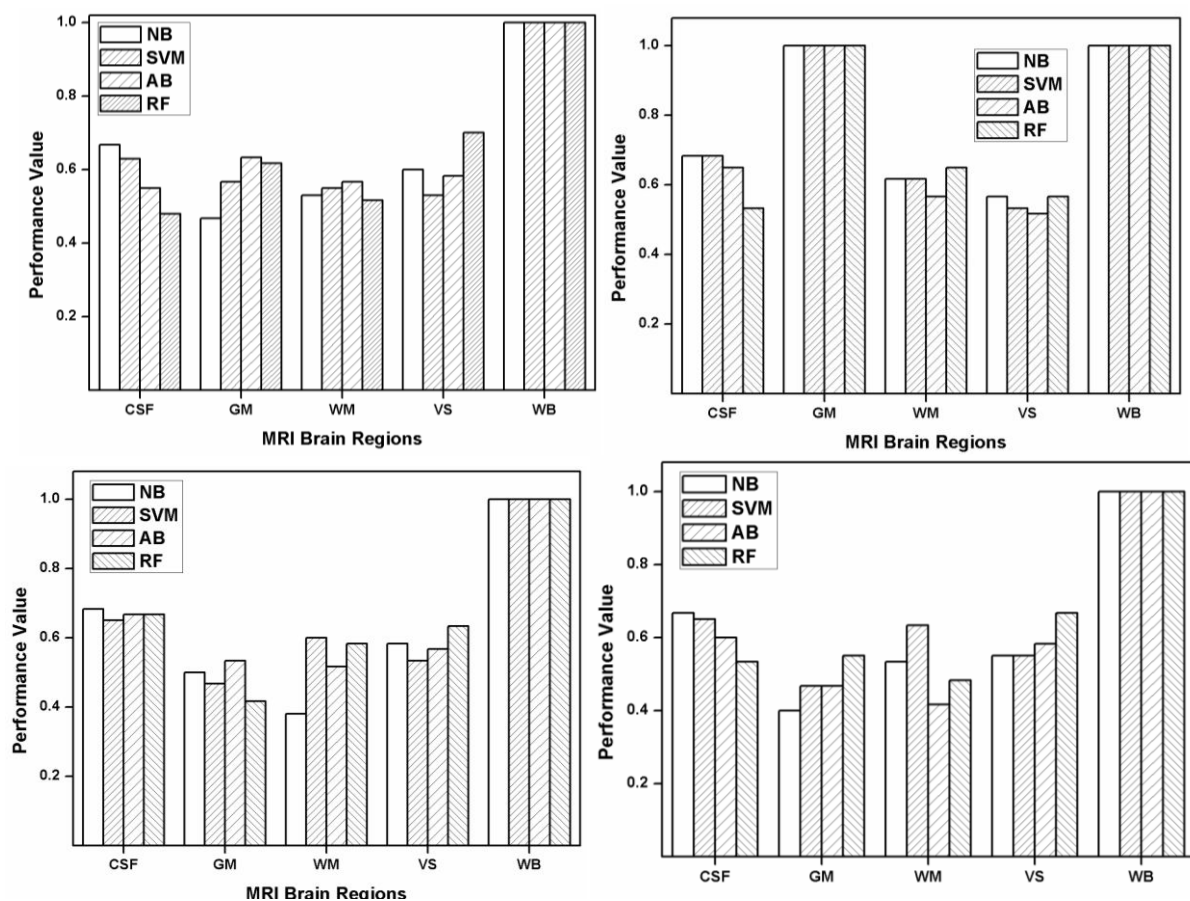
Figure-8. Accuracy measure of different classifiers in differentiating AD and MCI using (a) LBP (b) LTP (c) LMEBP and (d) LTrP features.

All local patterns could capture the variations in the texture details which may be due to rich texture information in those regions. This helps to classify AD and MCI with maximum accuracy of 100%. Gray matter shows the next highest accuracy of 100% using LTP features followed by CSF region using LMEBP features. On an average, LBP features show a classification performance of greater than 65% in all regions in differentiating AD and MCI subjects. The average performance of classifiers is observed to vary between 60 to 75% in differentiating MCI and Normal as shown in Figure-9.

www.arpnjournals.com
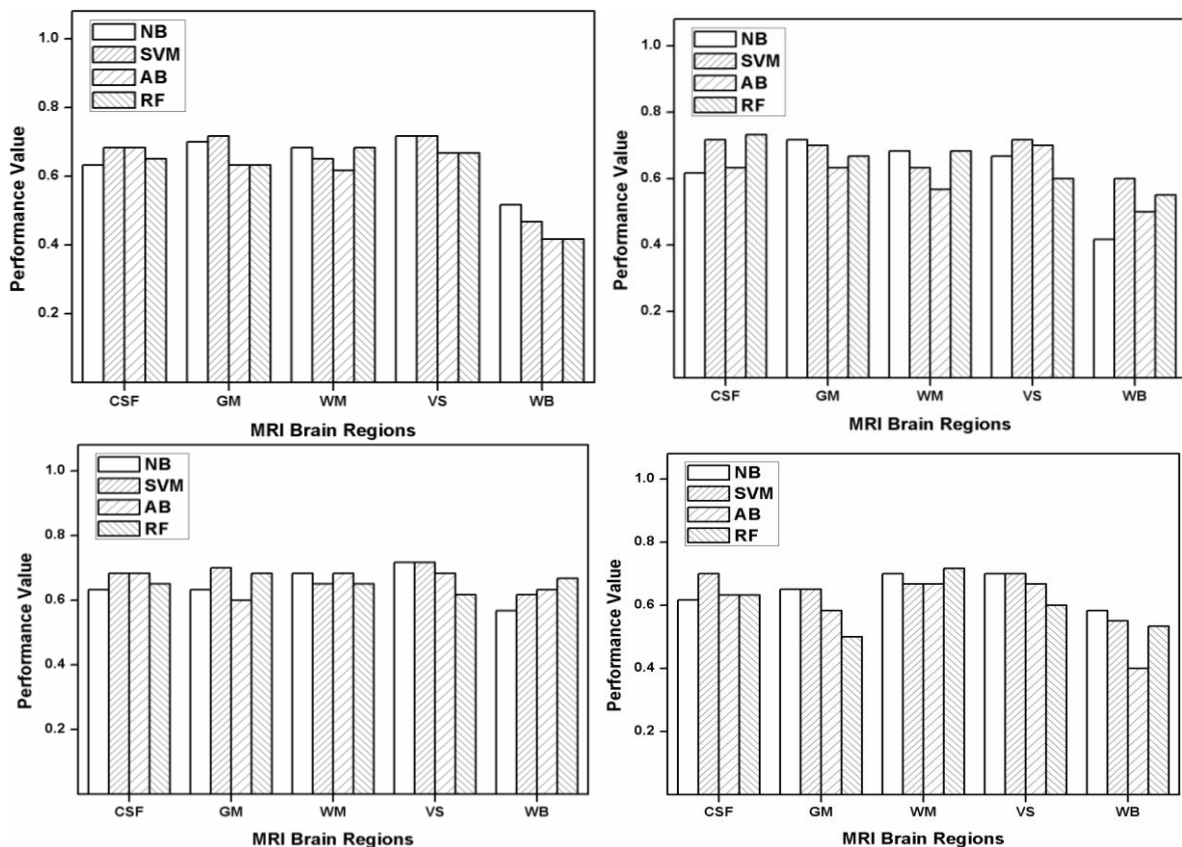
Figure-9. Accuracy measure of different classifiers in differentiating MCI and Normal using
(a) LBP (b) LTP (c) LMEBP and (d) LTrP features.

This shows that the structural variations are not significant as the disease progresses from normal to MCI. LMEBP based feature vector results in maximum accuracy of 73% for CSF regions using random forest classifier. The classification performance show a consistent results in classifying MCI and Normal especially for CSF, GM and ventricle regions of brain. There seems to be significant decrease in performance accuracy for whole brain region when compared to AD vs MCI which may be due to existence of negligible texture variations between MCI and normal subjects. Table-2 shows the results obtained in classifying MCI and Normal using LMEBP feature vector and SVM classifier. It is observed that an average performance greater than 65% is achieved using the proposed feature sets.

Table-2. Classification results using SVM and LMEBP features for differentiating
Normal and MCI.

	CSF	GM	WM	VS	WB
Accuracy	0.69	0.7	0.65	0.617	0.717
Sensitivity	0.657	0.714	0.645	0.63	0.689
Specificity	0.72	0.688	0.655	0.606	0.76

The classification performance in differentiating AD and normal subjects is shown in Fig. 10 for LBP, LTP, LMEBP and LTrP feature set using different classifiers. It is observed that the classification performance of AD and Normal subjects seems to be better than AD vs MCI and MCI vs Normal subjects in all brain tissue regions. This may be due to the increase in the disease severity as it progresses from normal to AD. The maximum performance is achieved using the features that are extracted from WB, GM and ventricle regions for LTP feature set. The other regions show a significantly good performance in classifying AD and Normal subjects. This shows that the local patterns are efficient to bring out the texture difference that is attributed due to severe disease condition. LTP feature vector is highly significant in classifying AD and Normal in CSF and Ventricle regions also.

www.arpnjournals.com
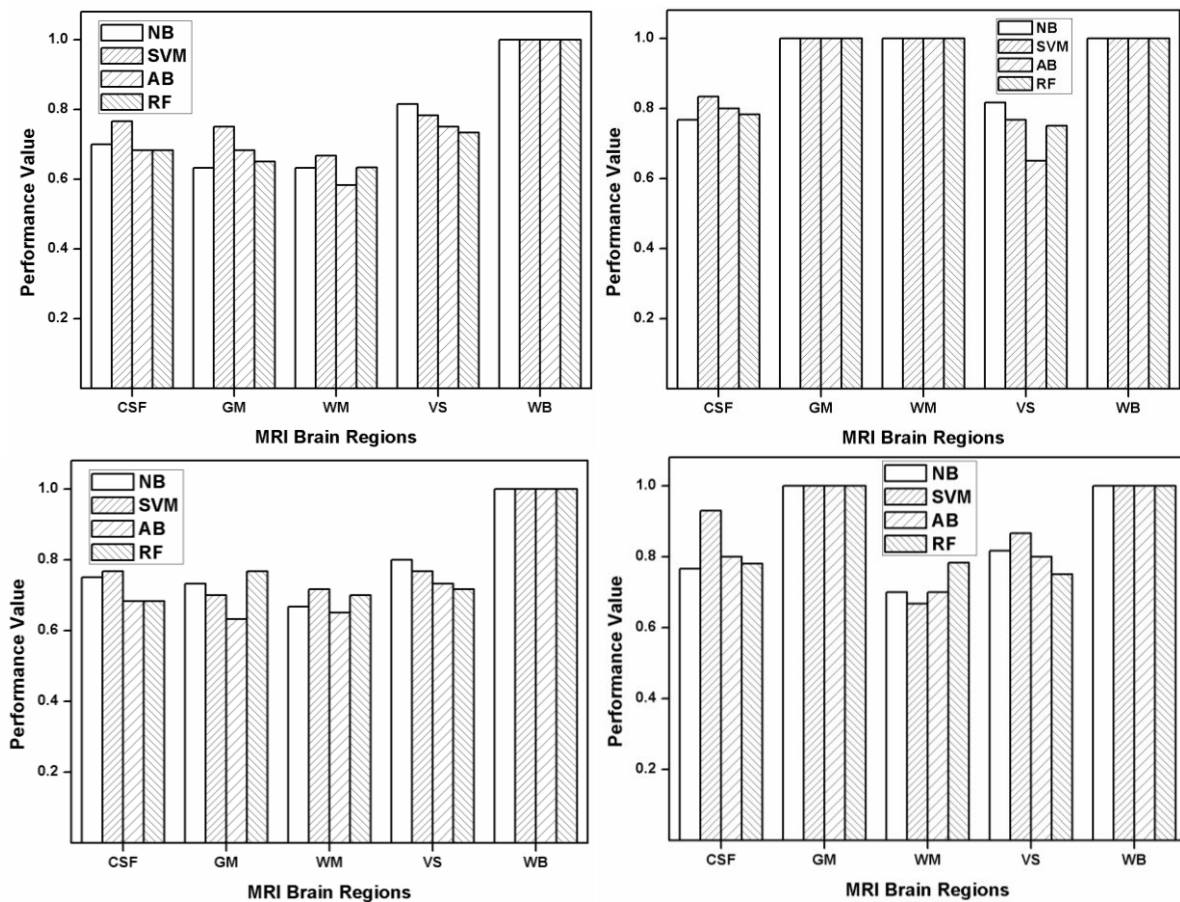
Figure-10. Accuracy measure of different classifiers in differentiating AD and Normal using
(a) LBP (b) LTP (c) LMEBP and (d) LTrP features.

Table-3 represents the performance measures of various regions of brain tissues in differentiating AD and Normal using LTP feature sets and SVM classifier. When compared to ADvsMCI and MCIvs Normal classification results, a consistent improvement in classification performance is observed. An average of 90% classification performance indicates that the LTP feature vector are efficient in differentiating the brain tissues by capturing the variations introduce due to tissues losses when the decrease progressed from Normal to AD. A significant improvement in performance is observed almost in all brain regions.

Table-3. Classification results using SVM and LTP features in differentiating
Normal and AD subjects.

	CSF	GM	WM	VS	WB
Accuracy	0.833	1	1	0.767	1
Sensitivity	0.763	1	1	0.711	1
Specificity	0.955	1	1	0.864	1

Figure-11 shows the performance results obtained in classifying AD, MCI and Normal subjects of various brain tissue regions using feature sets extracted from the corresponding local patterns. It is found that LTP feature set and SVM results in maximum accuracy of 82.2% in GM brain tissue region. Also it is observed that brain regions like GM and WB show a significant improvement by an average measure greater than 70% using LTP feature sets. WB region shows consistent performance in classifying AD, MCI and Normal subjects using all local patterns on an average measure greater than 67%. The structural variations in the brain tissues of various regions due to losses or shrinkages are efficiently captured by local ternary patterns.

www.arpnjournals.com
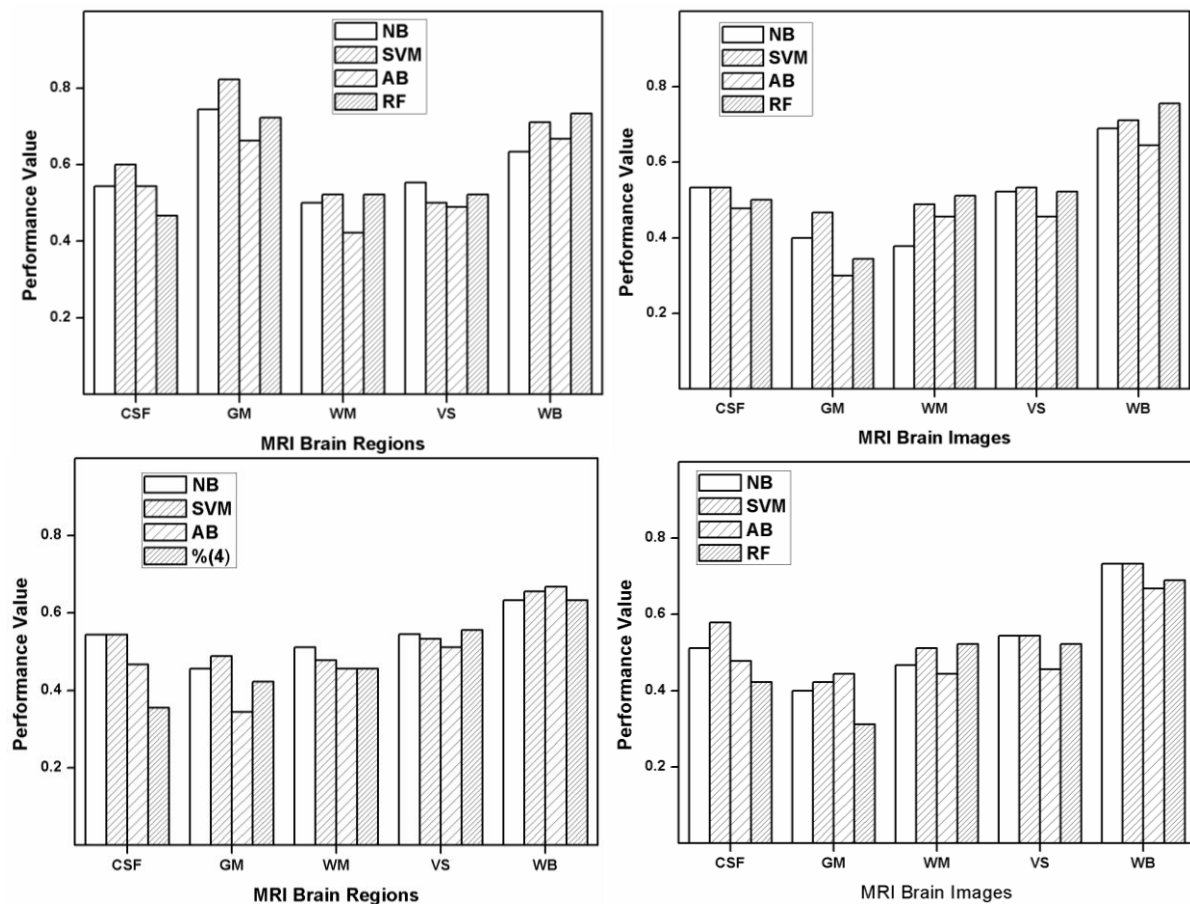
Figure-11. Performance of different classifiers in differentiating AD, MCI and Normal using
(a) LBP (b) LTP (c) LMEBP and (d) LTrP features.

Table-4 shows the classification accuracy of LTP feature sets derived from different brain tissues and different classifiers. It is found that LTP features extracted from GM and WB regions could show significant performances in classifying AD, MCI and normal subjects. In other regions, the performance is poor which may be due to insignificant variations in the intensity levels in those regions.

Table-4. Classification accuracy in differentiating AD, MCI and normal subjects using
different classifiers and different brain regions using LTP feature sets.

	CSF	GM	WM	VS	WB
NB	O.544	0.7444	0.50	0.511	0.7556
SVM	0.600	0.822	0.52	0.500	0.711
AB	0.544	0.662	0.42	0.4889	0.667
RF	0.4667	0.722	0.52	0.522	0.7333

4. CONCLUSIONS

In this work, regional atrophy analysis of Alzheimer MR brain images is carried out. Brain MR images are subjected to FCM based Anisotropic diffusion filter based level set framework in order to extract the various brain regions like gray matter (GM), white matter (WM), cerebrospinal fluid (CSF) and ventricle segment (VS). Local patterns such as local binary pattern (LBP), local ternary patterns (LTP), local maximum edge binary patterns (LMEBP) and local tetra patterns (LTrP) of

segmented brain regions are calculated. From each patterns, histogram based features are extracted and feature vectors are formed. The significance of the extracted features are analyzed by classifying the MR images into AD, MCI and normal subjects. The segmentation results show that the proposed automated algorithms could able to extract the various brain regions efficiently. The initial segmentation results obtained using FCM and anisotropic diffusion filtered edge map are able to drive the level set contour towards the desired

boundaries. The various local patterns of these segmented brain tissues are found to be significant in bringing out the edge details incorporating the textural variations. The classification accuracy in differentiating AD and normal seems to be high when compared to other cases resulting in maximum accuracy of 100 % using LTP features and SVM classifier in GM, WM and WB regions. Similarly, combination of SVM classifier and LTP features results in maximum accuracy of 82% in differentiating AD, MCI and normal subjects especially in GM brain regions. Thus, it appears that LTP features can be one of efficient biomarkers in identifying AD, MCI and Normal subjects. And also, the pipeline of FCM - ADLSM segmentation, LTP features of GM, WM, and WB regions with SVM classifier may improve the diagnostic relevance in automated diagnosis of Alzheimer disease using brain MR images.

REFERENCES

[1] World Health Organization. 2012. Dementia: Fact Sheet no. 362. Retrieved.

[2] Jack CR, Shiung MM, Weigand SD, O'Brien PC, Gunter JL, Boeve BF, Knopman DS, Smith GE, Ivnik RJ, Tangalos EG, Petersen RC. 2005. Brain atrophy rates predict subsequent clinical conversion in normal elderly and amnestic mci. Neurology. 65(8):1227-1231.

[3] Douglas G, Klauber MR, Hofstetter CR, Salmon DP, Lasker B, Thal LJ. 1990. The mini-mental state examination in the early diagnosis of alzheimer's disease. Arch Neurol. 47(1): 49-52.

[4] Albert MS, DeKosky ST, Dickson D, Dubois B, Feldman HH, Fox NC, Gamst A, Holtzman DM, Jagust WJ, Petersen RC, Snyder PJ, Carrillo MC, Thies B, Phelps CH. 2011. The diagnosis of mild cognitive impairment due to alzheimer's disease: recommendations from the national institute on aging-alzheimer's association workgroups on diagnostic guidelines for alzheimer's disease. Alzheimers Dement. 7(3): 270-279.

[5] Wisniewski HM, Wegiel J. 1995. Neuropathology of Alzheimer's disease. Neuroimaging Clin N Am. 5: 45-57.

[6] Rewcastle NB. 1991. Neurodegenerative disease. In: Davis RL, Robertson DM, eds. Textbook of Neuropathology. Baltimore, Md: Williams and Wilkins. pp. 908-919.

[7] Braak H, Braak E. 1991. Neuropathological staging of Alzheimer-related changes. Acta Neuropathol. 82: 239-259.

[8] Gado M, Hughes CP, Danziger W, et al. 1983. Aging, dementia, and brain atrophy: a longitudinal computed tomographic study. AJNR Am J Neuroradiol. 4: 699-702.

[9] Tanabe JL, Amend D, Schuff N, DiSclafani V, Ezekiel F, Norman N, Fein G, Weiner MW. 1997. Tissue segmentation of the brain in Alzheimer disease. AJNR Am J Neuroradiol. 18(1): 115-123.

[10] Farzan A, Mashohor S, Ramli AR, Mahmud R. 2014. Anatomical Analysis of Brain MRI in Alzheimer's disease. Proc International Conf Adv Engg Tech. 10-15.

[11] Nestor SM, Rupsingh R, Borrie M, Smith M, Accomazzi V, Wells JL, Fogarty J, Bartha R, ADNI. 2008. Ventricular enlargement as a possible measure of Alzheimer's disease progression validated using the Alzheimer's disease neuroimaging initiative database. Brain. 131(9): 2443-2454.

[12] Luca F, Palm WM, Olofsen H, Landen Rv, Buchem MA, Reiber JHC, Behloul FA. 2008. Ventricular shape biomarkers for Alzheimer's disease in clinical MR images. Magn Reson Med. 59(2): 260-267.

[13] Brun A, Englund EA. 1986. White matter disorder in dementia of the Alzheimer type: a pathoanatomical study. Ann Neurol. 19: 253-262.

[14] Zhang L, Raymond CC, Leung WC, Henry KFM. 2012. Current neuroimaging techniques in Alzheimer's disease and applications in animal models. Am J Nucl Med Mol Imaging. 2(3): 386.

[15] Teipel SJ, Grothe M, Lista S, Toschi N, Garaci FG, Hampel H. 2013. Relevance of magnetic resonance imaging for early detection and diagnosis of Alzheimer disease. Med Clin North Am. 97(3): 399-424.

[16] Mahanand BS, Suresh S, Sundararajan N, Aswatha KN. 2012. Identification of brain regions responsible for Alzheimer's disease using a Self-adaptive Resource Allocation Network. Neual Networks. 32: 313-322.

ARPN Journal of Engineering and Applied Sciences

[17] Lorena B, Rossi R, Testa C, Geroldi C, Galluzzi S, Laakso MP, Beltramello A, Soininen H, Frisoni GB. 2005. Visual assessment of medial temporal atrophy on MR films in Alzheimer's disease: comparison with volumetry. Aging Clin Exp Res. 17(1): 8-13.

[18] Teipel SJ, Bayer W, Alexander GE, Bokde ALW, Zebuhr Y, Teichberg D, Spahn FM, Schapiro MB, Möller HJ, Rapoport SI, Hampel H. 2003. Regional pattern of hippocampus and corpus callosum atrophy in Alzheimer's disease in relation to dementia severity: evidence for early neocortical degeneration. Neurobiol Aging. 24(1): 85-94.

[19] Killiany RJ, Hyman BT, Gomez-Isla T, Moss MB, Kikinis R, Jolesz F, Tanzi R, Jones K, Albert MS. 2002. MRI measures of entorhinal cortex vs hippocampus in preclinical AD. Neurology. 58(8): 1188-1196.

[20] Arno K, Andersson J, Ardekani BA, Ashburner J, Avants B, Chiang MC, Christensen GE, Collins DL, Gee J, Hellier P, Song JH, Jenkinson M, Lepage C, Rueckert D, Thompson P, Vercauteren T, Woods RP, Mann JJ, Parsey RV. 2009. Evaluation of 14 nonlinear deformation algorithms applied to human brain MRI registration. Neuroimage. 46 (3): 786-802.

[21] Olivier C, Chételat G, Chupin M, Desgranges B, Magnin B, Benali H, Dubois B, Garnero L, Eustache F, Lehéricy S. 2008. Discrimination between Alzheimer Disease, Mild Cognitive Impairment, and Normal Aging by Using Automated Segmentation of the Hippocampus 1. Radiology. 248(1): 194-201.

[22] Desikan RS, Cabral HJ, Hess CP, Dillon WP, Glastonbury CM, Weiner MW, Schmansky NJ, Greve DN, Salat DH, Buckner RL, Fischl B, ADNI. 2009. Automated MRI measures identify individuals with mild cognitive impairment and Alzheimer's disease. Brain: awp123.

[23] Paola DM, Macaluso E, Carlesimo GA, Tomaiuolo F, Worsley KJ, Fadda F, Caltagirone C. 2007. Episodic memory impairment in patients with Alzheimer's disease is correlated with entorhinal cortex atrophy. Journal of neurology. 254 (6): 774-781.

[24] Freeborough PA, Fox NC. 1998. Modeling brain deformations in Alzheimer disease by fluid registration of serial 3D MR images. J Comput Assist Tomogr. 22(5): 838-843.

[25] Tomoharu K, Kodama N, Shimada T, Fukumoto I. 2002. Application of run length matrix to magnetic resonance imaging diagnosis of Alzheimer-type dementia. Nihon Hoshasen Gijutsu Gakkai Zasshi. 58(11): 1502-1508.

[26] Devrim U, Ekin A, Cetin M, Jasinschi R, Ercil A. 2007. Robustness of local binary patterns in brain MR image analysis. Proc IEEE Eng Med Biol Soc. 2098-2101.

[27] Oppedal K, Engan K, Aarsland D, Beyer M, Tysnes OB, Eftestøl T. 2012. Using local binary pattern to classify dementia in MRI. Proc IEEE International Symposium Biomedical Imaging. 594-597.

[28] Oppedal K, Eftestøl T, Engan K, Beyer MK, Aarsland D. 2015. Classifying dementia using local binary patterns from different regions in magnetic resonance images. Int J Biomed Imaging.

[29] Ali BM, Ramli AR, Saripan MI, Mashohor S. 2010. Review of brain MRI image segmentation methods. Artif Intell Rev. 33(3): 261-274.

[30] ZhangbH, Yushkevich PA, Alexander DC, Gee JC. 2006. Deformable registration of diffusion tensor MR images with explicit orientation optimization. Med Image Anal. 10(5): 764-785.

[31] Suganthi SS, Ramakrishnan S. 2014. Anisotropic diffusion filter based edge enhancement for segmentation of breast thermogram using level sets. Biomed Signal Process Control. 10: 128-136.

[32] Anandh KR, Sujatha CM, Ramakrishnan S. 2014. Segmentation of ventricles in alzheimer mr images using anisotropic diffusion filtering and level set method. Biomed Sci Instrum. 50: 307-313.

[33] Anandh KR, Sujatha CM, Ramakrishnan S. 2014. Atrophy analysis of corpus callosum in Alzheimer brain MR images using anisotropic diffusion filtering and level sets. Proc IEEE Eng Med Biol Soc. 1945-1948.

[34] Prashant S, Bhadauria HS, Singh A. 2014. Automatic brain MRI image segmentation using FCM and LSM. Proc IEEE conf Reliability, Infocom Technologies and Optimization. 1-6.

[35] Ammara M, Jumaily AAA. 2013. Fuzzy C mean thresholding based level set for automated

segmentation of skin lesions. Journal of Signal and Information Process. 4(3): 66.

[36] Ghalehnovi M, Zahedi E, Fatemizadeh E. 2014. Integration of spatial fuzzy clustering with level set for segmentation of 2-D angiogram. Proc IEEE Conf Biomed Engg and Scien. pp. 309-314.

[37] Daniel MS, Wang TH, Parker J, Csernansky JG, Morris JC, Buckner RL. 2007. Open Access Series of Imaging Studies (OASIS): cross-sectional MRI data in young, middle aged, nondemented, and demented older adultsJ Cogn Neurosci. 19(9): 1498-1507.

[38] Li C, Xu C, Gui C, Fox MD. 2005. Level set evolution without re-initialization: a new variational formulation.   Proc IEEE Comp Society Conf Computer Vision and Pattern Recog. 1: 430-436.

[39] Chuang KS, Tzeng HL, Chen S, Wu J, Chen TJ. 2006. Fuzzy c-means clustering with spatial information for image segmentation.   Comput Med Imaging Graph. 30(1): 9-15.

[40] Ojala T, Pietikainen M, Maenpaa T. 2002. Multiresolution gray-scale and rotation invariant texture classification with local binary patterns. IEEE Trans. Pattern Anal. Mach. Intell. 24(7): 971–987.

[41] Subrahmanyam M, Maheshwari RP, Balasubramanian R. 2012. Local maximum edge binary patterns: a new descriptor for image retrieval and object tracking. Signal Process. 92(6): 1467-1479.

[42] Tan X, Triggs B. 2010. Enhanced local texture feature sets for face recognition under difficult lighting conditions. IEEE T Image Process. 19(6): 1635-1650.

[43] Subrahmanyam M, Maheshwari RP, Balasubramanian R. 2012. Local tetra patterns: a new feature descriptor for content-based image retrieval. IEEE T Image Process. 21(5): 2874-2886.

[44] Archana C, Mali SN. 2014. Evaluation of texture and shape features for classification of four paddy varieties. Journal of Engineering. pp. 1-8.